Article

Bipolar Electrode based Multi-Color Electrochemiluminescence Biosensor

Yinzhu Wang, Cong-Hui Xu, Wei Zhao, Qi-Yuan Guan, Hong-Yuan Chen, and Jing-Juan Xu

Anal. Chem., **Just Accepted Manuscript** • DOI: 10.1021/acs.analchem.7b01494 • Publication Date (Web): 29 Jun 2017

Bipolar Electrode based Multi-Color Electrochemiluminescence Biosensor

Yin-Zhu Wang, Cong-Hui Xu, Wei Zhao, Qi-Yuan Guan, Hong-Yuan Chen, Jing-Juan Xu**

State Key Laboratory of Analytical Chemistry for Life Science and Collaborative Innovation Center of Chemistry for Life Sciences, School of Chemistry and Chemical Engineering, Nanjing University, Nanjing 210023, China.

* Corresponding author. Tel/Fax: +86-25-89687294; E-mail address: weizhao@nju.edu.cn (W. Zhao) xujj@nju.edu.cn (J.J. Xu)

ABSTRACT:

We report a multi-color ECL device based on closed bipolar electrode (BPE) for the visualized sensing of prostate-specific antigen (PSA) in human blood serum. As the emission color of concomitant electrochemiluminophores is potential resolved, similar to a three-electrode system, selective excitation of ECL could be achieved by tuning the interfacial potential at the poles of BPE. Via modulating the resistance of BPE, multi-color ECL emission of $[Ru(bpy)_3]^{2+}$ and $[Ir(ppy)_3]$ mixture using tripropylamine (TPrA) as the co-reactant was observed at the anode and the principle was elaborated. The concept was utilized to the quantification of clinical biomarkers with the color variation. A PSA concentration dependent silver bridge was constructed in the gap of the BPEs as an electric conductivity modulator. On the basis of multi-color BPE-ECL device, the cut-off values (4.0 ng/ml and 10.0 ng/ml) of human PSA could be recognized by the green-yellow-red ECL emission changing with naked eyes. As the first multi-color ECL device in biological analysis, BPE may raise the application of potential-resolved ECL to a new level.

KEYWORDS: Multi-Color, Electrochemiluminescence, Bipolar electrode, $[Ru(bpy)_3]^{2+}$, $[Ir(ppy)_3]$, Prostate-specific antigen.

INTRODUCTION

Electrochemiluminescence (ECL) is an electrochemically initiated chemiluminescence process, in which molecules or quantum dots are oxidized or reduced at the surface of electrode, to form photon emitting state, leading to luminescence upon return to the ground state.[1~9] As excitation processes of ECL fundamentally depends on energy of the excited state, multiple electrochemiluminophores can be distinguished by not only their wavelengths of the emission, but also the voltages required for the excitation.[10~14] Multi-color ECL systems, accordingly, have emerged as a powerful tool for the simultaneous detection of spectrally distinct electrochemiluminophores, and study of electron transfer pathways via manipulating the applied potentials.[15~17] The ruthenium (II) and iridium (III) complexes with tripropylamine (TPrA) as a co-reactant show emission maxima spanning the whole visible region, thereby incorporating these two types of complexes, impressive works have been reported towards the color-tunable ECL devices.[18~19]

Despite the important development in this area, application of visualized multi-color ECL devices in biological analysis is limited, which is a pity since the most important application of the remarkably sensitive ECL detection system is immunoassay in the clinical practice. It is not surprising since most Ru and Ir complexes are insoluble in aqueous solution, which limits their biological application. In recent years, we reported several bipolar electrode (BPE) based devices using ECL as an optical reporter.[20~22] Generally, a bipolar electrode is an electrically conductive material that immerses in an electrolyte which promotes electrochemical reactions at its extremities under sufficient driving voltage.[23] The system was defined as “open” BPE with existence of both electronic and ionic current paths. Another design which was called as split-channel BPE or “closed” BPE physically separates the solutions contacting the anode and cathode of the BPE, with only

current path between the two half cells. Such BPE systems hold promise for the fabrication of colorimetric ECL biosensor since ECL reactions process in a separated cell.[24~25] Similar to the traditional three-electrode system, interfacial potential difference between the pole of the BPE and the solution drives the ECL reactions.[26] As the interfacial potential could be easily modulated in the BPE system, we suppose the potential resolved multi-color emission ECL processes could be realized in closed BPE based device.

Herein, we built a closed BPE based multi-color ECL sensor using a mixture of $[Ru(bpy)_3]^{2+}$ and $[Ir(ppy)_3]$, the red and green luminophores as the multi-color emitters and TPrA as the co-reactant. Through altering the resistance of BPE, a three-color change (green-yellow-red) was observed at the anode, indicating that BPE could indeed be exploited for the development of color selected ECL devices. Further, we proposed an application of fast screening of the clinical biomarker, prostate-specific antigen (PSA), via PSA guided deposition of silver particles which regulated the electronic conductivity of BPE. Currently, 4.0 ng/mL PSA in blood serum is considered as the cut-off value for prostatic diseases.[27] And PSA level exceeds 10.0 ng/mL is highly considered for biopsy to diagnose prostate cancer. A multi-color visualization method should be suitable for identifying the levels of PSA in blood serum for both the early diagnosis and the prognosis evaluation. Via the varied emissions of multiple electrochemiluminophores that resulted in different colors, PSA concentrations in different zones could be recognized directly by naked eye. Real blood serum sample tests proved the feasibility and reliability of the proposed multi-color ECL sensor. Such closed BPE device may greatly expand the applications of potential resolved colorimetric ECL.

EXPERIMENTAL SECTION

Fabrication of closed BPE. A piece of ITO was first cut into small slices (6.5 cm*1 cm) and fabricated on a silk-screen. For screen-printing, oil ink (essential ingredient of acrylic resin) was transmitted through the silk-screen onto the ITO layer. Once the planar electrodes were completed, a wet chemical etching procedure was carried out with chemical solution (HF: NH_4F: HNO_3=1: 0.5: 0.5), which produced the desired ITO electrodes (driving electrode:1.5 cm in length, 1.5 cm in width; the two split BPEs: 1 cm in length, 0.5 mm in width； a gap of the BPEs with space of 1.5 mm). Those ITO electrode slices were cleaned by immersion in a boiling solution of 2 M KOH in 2-propanol for 20 min, followed by washing with milli-Q water. To obtain the PDMS molds, SG-2506 borosilicate glass was fabricated by traditional photolithography and wet chemical etching techniques. SG-2506 borosilicate glass plates were exposed to UV radiation under a mask with the designed patterns, followed by developing with a 0.5% NaOH solution, the Cr layer was then removed by a 0.2 M ammonium cerium (IV) nitrate solution. Etching of these glass plates was carried out in 1 M HF-NH_4F solution (40 ˚C) with a water bath for 28 min. After that, designed channel structures molds were obtained. Then degassed PDMS was cast on these glass masks for 1 h in 80 ˚C. After cooling at room temperature, the PDMS was stripped from the masks, producing the PDMS microfluidic channel (1 cm in length, 1.8 mm in width, 45 μm in depth) and PDMS reservoir mode with holes of 4 mm in diameter.

Surface pretreatment of the gap. The ITO slices were immersed into 1 M NaOH for 4 h to ensure the presence of hydroxyl groups. Then the hydrophilic surface of the gap was functionalized with APTES by immersing in a 2% (v/v) ethanol solution of APTES at 4 ˚C for 12 h, and rinsed three times with ethanol and heated at 120 ˚C for 30 min. Covering by PDMS channel, the gap of BPEs

was incubated with 20 μL glutaraldehyde (2.5%) at 37 ˚C for 1 h, followed by rinsing with phosphate buffer solution (PBS, pH=7.4) thoroughly. Finally, 20 μL of 20 mg/mL primary anti-PSA antibody (Ab1) was introduced to the gap at 37 ˚C for 3.5 h. After carefully rising with PBS, the prepared ITO slices were stored at 4 ˚C for further use.

Microfluidic sampling. The sampling was proceeded automatically (Scheme 3). Firstly, a series of reagents manually using a 1 mL syringe to draw reagents into the PE tube (0.7 mm ID, 1.0 mm OD). We separate the reagent plugs with air spacers each of 0.5 cm in length. The reagent sequence consists one plug of PSA in 1% BSA/0.05% Tween-20 in filtered PBS (1.5cm, 5.8 μL), four small plugs of washing buffer (0.3 cm, 1.2 μL), one plug (2.5 cm, 9.6 μL) of gold nanoparticle-conjugated PSA antibody2 (Ab2) (1.45 μg/mL in 3% BSA/0.2% Tween-20 in filtered PBS), two small plugs (0.3 cm, 1.2 μL) of washing buffer, four small plugs (0.3 cm, 1.2 μL) of distilled water, and one plug of silver reagent (3.0 cm, 11.6 μL). The flow rate was adjusted to 8 μL/min. The flow was stopped for 12 min when PSA and Ab2 were flowing through the gap for incubation, and for 3 min for the incubation of silver reagent. The overall flow-through process can be completed within 35 min.

After one test, the ITO slice was cleaned with alcohol cotton to wipe off metal nanoparticles in the gap. Then it was sonicated in water, ethanol, and water each for 5 min, and dried by nitrogen. Further the ITO slice was immersed in a boiling solution of 2 M KOH in 2-propanol for 15 min. Finally, it was rinsed with piranha solution and milli-Q water for the next use.

ECL measurements. Two instrumental systems were used for ECL measurements, the closed BPE system and three-electrode system with ITO glass as working electrode (3 mm in diameter), $Ag/AgNO_3$ as non-aqueous reference electrode, and a platinum wire as counter electrode. Luminophore solutions contained $[Ru(bpy)_3]^{2+}$, $[Ir(ppy)_3]$ and 25 mM TPrA as the coreactant. For

BPE based ECL experiments, ECL images were taken with Olympus DP71 cooled CCD camera, meanwhile the total currents were recorded. The ECL spooling spectra were obtained based on three-electrode system, and using CHI 660C combined with F700 fluorescence spectrometer (Hitachi, Japan). The integration time per spectrum was 10 s, the voltage resolution of the 3D matrix was 100 mV per spectrum. 3D data were smoothed and graphed using matlab analysis software. All experiments were carried out at room temperature.

RGB Analysis. Image J was used to automate the cropping and analysis of the images. Images were cropped to the smallest square area containing the emissive electrode areas, this resulted in a 100×100 pixel image. The mean RGB values were measured for the circular area of the electrode using the "Measure−RGB Values" function built into Image J.

HSV transformations of the RGB data were carried out using the following formulas:

M=max(R,G,B)

m=min(R,G,B)

if R = M, H' = (G-B)/(M-m)

if G = M, H' = 2 + (B-R)/(M-m)

if B = max, H' = 4 + (R-G)/(M-m)

H = H' * 60

S=(M-m)/M

V=max(R,G,B)

RESULTS AND DISCUSSION

Multi-color ECL of $[Ru(bpy)_3]^{2+}$ and $[Ir(ppy)_3]$. As preliminary experiments, conventional three-electrode ECL system comprising mixed organic luminophores of $[Ru(bpy)_3]^{2+}$ with red emission (λ_{max}=620 nm), and $[Ir(ppy)_3]$ (λ_{max}=517 nm) (Figure 1) were conducted to validate the ECL spectra and emission colors tuned by potential. The experiments were carried out by generating the radical ions of the two compounds sequentially via modulating the electrode potential. As shown in three-dimensional data sets of ECL intensity versus both emission wavelength and excitation potential (Figure 1), with the assistant of oxidative-reduction co-reactant, TPrA, the green emitter of $[Ir(ppy)_3]$ is selectively addressed at low oxidation potentials (0.4-0.8V vs. $Fc^{0/+}$). At potential of 0.9 V vs. $Fc^{0/+}$, red emitter of $[Ru(bpy)_3]^{2+}$ starts to be excited. At higher potentials (0.9-1.3 V vs. $Fc^{0/+}$), both emitters are observed, but they remain distinguishable by wavelengths. The results are similar to Richter's report of the ECL emission spectrum of the two metal complexes in the same solution.[28] We observed that at 0.8V, the emission color of the mixed 0.5 mM $[Ir(ppy)_3]$ and 0.75 mM $[Ru(bpy)_3]^{2+}$ showed pure green. At 1.1V, the red ECL of $[Ru(bpy)_3]^{2+}$ and green ECL of $[Ir(ppy)_3]$ combined as a yellow emission. At higher potential of 1.3V, red emission dominated. The green-yellow-red color variations are the most eye-catching. The colors were firstly observed with naked eye, then photographs of ECL at three electrode potentials were taken by CCD camera. It should be noted that the ECL emission of $[Ir(ppy)_3]$ was generally suppressed at high overpotentials, which could be attributed to the oxidative quenching of $[Ir(ppy)_3]$* by the TPrA radical cation,[15, 19, 29] which was called as the ECL 'switch-off' phenomenon. Therefore, the concentration of TPrA was optimized in the first place. As shown in Figure S1, at 1.1 V vs. ferrocene/ferrocenium couple, the green ECL emission got brighter when TPrA concentration increased from 5 mM to 25 mM, but

turned dark with 50 mM TPrA. With higher amount of TPrA, the quenching of $[Ir(ppy)_3]$* by the TPrA radical cation dominated the ECL emission efficiency of $[Ir(ppy)_3]$. The concentration of TPrA was optimized as 25 mM.

BPE based multi-color ECL. No matter at the working electrode in a traditional three-electrode system or the poles of BPE, it is the interfacial potential difference ($\Delta\phi$) drives the oxidation and reduction reactions. Herein, a closed BPE (Scheme 1A) was adopted for the demonstration of multi-color ECL. As there are four electrode/solution interfaces in a closed-BPE system, from the potential profile (Scheme 1B) through the whole electrochemical cell, it was recognized that the potential applied on the cell equals to the sum of the four interfacial potential differences ($\Delta\phi_a$, $\Delta\phi_c$, $\Delta\phi_a'$, $\Delta\phi_c'$) and potential dropped on the solutions and BPE. At the anodic pole of the BPE, the anodic interfacial potential difference $\Delta\phi_a$ drives the ECL reactions. The equivalent circuit of the anodic interface is shown in the enlarged figure of Scheme 1, which contains a double-layer capacitance represented by the element C_d, and a general impedance Z_f indicating the faradaic process. When faradaic reactions occur at the BPE, the total current (i_{tot}) through the working interface is the sum of distinct contributions from the faradaic process, i_f, and double-layer charging, i_c. Settling the amount of reactants and geometry of the BPE, increase of i_{tot} should result in higher overpotential (η) at the poles (Tafel equation, Eq. 1).[30]

$$\eta = a + b\lg i \quad (1)$$

As $\Delta\phi_a$ is in positive relation with η, $\Delta\phi_a$ at the anodic interface could be regulated by i_{tot}, which depends on several factors, for instance, E_{tot}, the resistance of BPE and the concentration of the reactants. In other words, via adjusting specific factor, $\Delta\phi_a$ should be varied and lead to the change

of kinetics of faradic reactions occurring at the surface of BPE. $\Delta\phi$ for a single interface is hard to be measured using traditional method.[30] Very recently, Wang's group published a work using surface plasmon resonance microscopy (SPRM) to mapping the interfacial potential distribution on bipolar electrode arrays.[31] It enabled the quantification of the absolute potential over the electrode surfaces. However, it relied on gold film with unique optical character.

Detection principle. Multiple electrochemiluminophores with different emission colors enable more intuitive observation of potential variation at the BPE interface. An emission color tunable device could be fabricated based on BPE similar to the potential resolved three-electrode system. According to this concept, we fabricated a closed BPE device with variable BPE resistance as a modulator of the $\Delta\phi_a$, and Ru and Ir complexes of $[Ru(bpy)_3]^{2+}$ and $[Ir(ppy)_3]$ were chosen as the ECL reporters. The fabrication process is shown in Scheme 2. Using wet chemical etching techniques, BPEs with a gap was formed and then connected with a variable resistor as a whole. PDMS molds with micro-channels covered at the ITO slide to form the anodic and cathodic reservoirs. A simplified scheme of the device is shown in Figure 2A. The mixture of 0.5 mM $[Ir(ppy)_3]$ and 0.75 mM $[Ru(bpy)_3]^{2+}$ with 25 mM TPrA as the co-reactant in acetonitrile containing 0.1 M $TBAPF_6$ was added in the anodic reservoir. The cathodic reservoir contained aqueous solution of 0.1 M phosphate buffer with 0.1 M NaCl. Under external potential of 5.5 V (E_{tot}), electrochemiluminophores were excited at the anode, accordingly, oxygen was reduced at the cathode. The conduction via BPE makes the reactions on the extremities electrically balanced. As the resistance of BPE was varied from 20 Ω to 0.1 M Ω, the i_{tot} decreased significantly (Figure 2C), and the color of the ECL emission changed from red to yellow and then green (Figure 2B). We may name the device as a BPE resistance resolved multi-color ECL system, which was very close to the proof-of-concept

experiment with three-electrode system under different potentials. Since the closed or split-channel BPEs based ECL sensors hold a specialty to separate solutions contacting the BPE anode and cathode physically, aqueous and organic solvents could be used in the system, which benefits the application of ECL in organic phase, especially the multi-color ECL system based on Ru and Ir complexes.

On the basis of the BPE resistance resolved ECL emission, a PSA guided silver bridge was deposited in the gap of two BPEs as an electric conductivity modulator (Scheme 3, Figure 3A). In brief, it was based on a immunosorbent assay, where primary anti-PSA antibody (Ab1) were firstly covalently bound at the gap between the ITO bands by glutaradehyde, then PSA and Au NPs labelled PSA antibody (Ab2) were captured on the surface respectively. Finally silver enhancement solution was introduced, and Ag particles deposited on AuNPs gradually spred out and linked the two ITO bands as a bridge. It should be emphasized that all these reagents except Ab1 were delivered automatically with microfluidic system (Scheme 3). The overall process could be completed within 30 min. After sandwich reaction and the formation of silver bridge, ITO slide was dried by nitrogen for ECL measurements. As shown in Figure S2, using standard PSA sample with concentration of 4.0 ng/ml, both ECL reactions of $[Ir(ppy)_3]$ and $[Ru(bpy)_3]^{2+}$ were excited with mixed emission color of yellow at 5.5 V driving voltage. With 1-10 min nitrogen sweeping, the itot of the system kept stable. However, if the ITO slide was baked in the oven under 120 ˚C for half an hour, i_{tot} dropped significantly and the emission color turned to dark green. As shown in Figure S3C, the silver bridge cracked at high temperature. Hence before each measurement, the BPE was simply dried with nitrogen for 1 min. Figure S3 shows the morphology of BPEs before and after the PSA guided silver deposition. The results showed the gap was smooth and clean without any treatment.

After sandwitch reaction and flow of silver reagents, there were large particles dispersed in the gap and connected two BPEs. Similiar to the variable resistor, the amount of Ag particles was positively related to the concentration of PSA, which could be utilized for the screening of PSA.

PSA sensing. Most doctors consider PSA level of 4.0 ng/ml as the cut-off value for possible prostate cancer.[27] Herein, on the basis of BPE based multi-color ECL device, we planned to set the 4.0 ng/ml as the "green to yellow" color changing point. To achieve the goal, the ratio of the concentration of $[Ru(bpy)_3]^{2+}$ to $[Ir(ppy)_3]$, the driving potential, as well as the inter space length of the gap were regulated (Figure S4-S6). As shown in Figure 3B, at driving potential of 5.5 V, the construction of silver bridge across 1.5 mm gap resulted in sequential changes in the ECL emission color of the mixture of 0.5 mM $[Ir(ppy)_3]$ and 0.75 mM $[Ru(bpy)_3]^{2+}$, depending on the concentration of PSA from 1.0 to 20.0 ng/ml. The color changing point of "green to yellow" appeared at 4.0 ng/ml. In addition, a "yellow to red" point appeared at 10.0 ng/ml. At this point, a prostate biopsy is highly recommended for the patients. The color variations were suitable for semi-quantitative assay. Spooling ECL spectra are shown in Figure 3C, the ECL intensities at wavelengths of 517 nm and 620 nm could both be adopted for precise quantification (Figure S7). We also measured the resistance of BPE and i_{tot} after the PSA guided silver deposition. As shown in Figure 3D, when the PSA concentration increased from 1.0 ng/ml to 10.0 ng/ml, the resistance decreased sharply, meanwhile i_{tot} increased significantly. While when the PSA concentration was larger than 10.0 ng/ml, both resistance and i_{tot} kept stable, which was consistent with the ECL color readout. The RGB analysis is a simple alternative approach for the multi-color ECL data processing. The ECL images were firstly split into three basic channels using ImageJ software (Figure S8). Figure S9 shows a HSV (Hue, Saturation, Value) representation of the color changes observed with the two

luminophores relying on the concentration of PSA. By monitoring changes in emission color (H coordinate) and emission intensity (V coordinate), quantitative information could be obtained.

The device to device variation was evaluated using six sensors, and 3 different PSA concentrations were measured (3.0 ng/ml, 5.0 ng/ml and 9.0 ng/ml). As shown in Figure S10, observed with naked eye, the consistency of the ECL emissions was perfect. For quantitative analysis, the RGB values of the ECL images were separated using matlab. Since the R value of ECL images with 3.0 ng/ml was too low, we adopted G value to determine the RSD of 3.0 ng/ml PSA detection using 6 different sensors as 3.10 %. And R/G value was applied to determine the RSD of 5.0 ng/ml and 9.0 ng/ml PSA analysis, which were 4.38%, 6.48%, respectively. The device could be reused after careful surface cleaning. The RSD of 5 times reuse of the device for the detection of 4.0 ng/ml PSA was 5.13%. The proposed sensor shows acceptable reproducibility.

To test the feasibility of proposed multi-color ECL-BPE sensor, a series of human blood serum sample with different concentrations of PSA (1.23-16.49 ng/mL) obtained from the Jiangsu Tumor Hospital were measured. As shown in Table 1, the colors of ECL emission fit well with the reference values provided by the hospital. The proposed BPE-ECL sensor could be applied for fast and intuitive judgement of the status of prospate disease, which is of great potential application in clinical diagnostics.

CONCLUSIONS

In summary, we developed a multi-color ECL sensor based on closed BPE device. Via modulating the resistance of the BPE, the color of emission of $[Ru(bpy)_3]^{2+}$ and $[Ir(ppy)_3]$ complexes mixture at the anode was finely tuned. Similar to the potential resolved ECL at three-electrode system, the

changes of interfacial potential at the electrode surface play a key role in selective excitation of the luminophores. As the ECL reactions processed in a separated reservoir of the closed BPE system, superior to three-electrode system, the multi-color ECL emission based on closed BPE system could be applied for bioanalysis. Here a PSA sensor was built based on the concept. After 35 min automatic sampling, we could easily identify the levels of PSA with the eye-catching color changes. In addition to the resistance-resolved ECL based on BPE, reactions at the cathode, which change the faradaic current flow through the BPE could also be monitored through the emission color readout at the anodic pole, and that will be our further research topic. Since arrays of BPEs can be controlled with just a single DC power supply or even a battery, we believe the multi-color ECL-BPE has promising usage in the screening of multiple analytes.

ACKNOWLEDGMENT

This work was supported by the Science and Technology Ministry of China (Grant No. 2016YFA0201200), the National Natural Science Foundation (Grants 21327902, 21535003) of China. This work was also supported by a Project Funded by the Priority Academic Program Development of Jiangsu Higher Education Institutions.

Supporting Information Available: The Supporting Information is available free of charge on the ACS Publications website.

Materials and apparatus, synthesis of Au nanoparticles labeled antibody 2, optimization of experiment parameters, SEM images of the gap between BPEs before and after silver deposition, ECL calibration curve, RGB analysis and reproducibility of the BPE-ECL device.

REFERENCES:

(1) Richter, M. M. *Chem. Rev*. **2004**, *104*, 3003-3036.

(2) Diez, I.; Pusa, M.; Kulmala, S.; Jiang, H.; Walther, A.; Goldmann, A. S.; Muller, A. H.; Ikkala, O.; Ras, R. H. *Angew. Chem*. **2009**, *48*, 2122-2125.

(3) Herbert, M. B.; Marx, V. M.; Pederson, R. L.; Grubbs, R. H. *Angew. Chem*. **2013**, *52*, 310-314.

(5) Rizzo, F.; Polo, F.; Bottaro, G.; Fantacci, S.; Antonello, S.; Armelao, L.; Quici, S.; Maran, F. *J. Am. Chem. Soc*. **2017**, *139*, 2060-2069.

(6) Xu, L.; Li, Y.; Wu, S.; Liu, X.; Su, B. *Angew. Chem*. **2012**, *51*, 8068-8072.

(7) Ishimatsu, R.; Matsunami, S.; Kasahara, T.; Mizuno, J.; Edura, T.; Adachi, C.; Nakano, K.; Imato, T. *Angew. Chem*. **2014**, *53*, 6993-6996.

(8) Dick, J. E.; Renault, C.; Kim, B. K.; Bard, A. J. *Angew. Chem*. **2014**, *53*, 11859-11862.

(9) Shan, D.; Qian, B.; Ding, S. N.; Zhu, W.; Cosnier, S.; Xue, H. G. *Anal. Chem*. **2010**, *82*, 5892-5896.

(10) Doeven, E. H.; Barbante, G. J.; Hogan, C. F.; Francis, P. S. *ChemPlusChem*. **2015**, *80*, 456 -470.

(11) Sun, W.; Sun, S.; Jiang, N.; Wang, H.; Peng, X. *Organometallics*. **2015**, *34*, 3385-3389.

(12) Zhang, H. R.; Xu, J. J.; Chen, H. Y. *Anal.Chem*. **2013**, *85*, 5321-5325.

(13) Zhang, H. R.; Wu, M. S.; Xu, J. J.; Chen, H. Y. *Anal.Chem*. **2014**, *86*, 3834-3840.

(14) Hesari, M.; Swanick, K. N.; Lu, J. S.; Whyte, R.; Wang, S.; Ding, Z. *J. Am. Chem. Soc.* **2015**, *137*, 11266-11269.

(15) Barbante, G. J.; Kebede, N.; Hindson, C. M.; Doeven, E. H.; Zammit, E. M.; Hanson, G. R.; Hogan, C. F.; Francis, P. S. *Chemistry*. **2014**, *20*, 14026-14031.

(16) Kerr, E.; Doeven, E. H.; Barbante, G. J.; Hogan, C. F.; Bower, D. J.; Donnelly, P. S.; Connell, T.

U.; Francis, P. S. *Chem. Sci*. **2015**, *6*, 472-479.

(17) Doeven, E. H.; Zammit, E. M.; Barbante, G. J.; Hogan, C. F.; Barnett, N. W.; Francis, P. S. *Angew. Chem*. **2012**, *51*, 4354-4357.

(18) Kerr, E.; Doeven, E. H.; Barbante, G. J.; Hogan, C. F.; Bower, D. J.; Donnelly, P. S.; Connell, T. U.; Francis, P. S. *Chem. Sci*. **2015**, *6*, 472-479.

(19) Doeven, E. H.; Barbante, G. J.; Kerr, E.; Hogan, C. F.; Endler, J. A.; Francis, P. S. *Anal. Chem*. **2014**, *86*, 2727-2732.

(20) Wu, M. S.; Yuan, D. J.; Xu, J. J.; Chen, H. Y. *Chem. Sci*. **2013**, *4*, 1182.

(21) Wu, M. S.; Liu, Z.; Shi, H. W.; Xu, J. J.; Chen, H. Y. *Anal. Chem*. **2015***, 87*, 530-537.

(22) Zhang, H. R.; Wang, Y. Z.; Zhao, W.; Xu, J. J.; Chen, H. Y. *Anal. Chem*. **2016**, *88*, 2884-2890.

(23) Chow, K. F.; Mavré, F.; Crooks, R. M. *J. Am. Chem.Soc*. **2008**, *130*, 7544-7545.

(24) Wu, M. S.; Yuan, D. J.; Xu, J. J.; Chen, H. Y. *Anal. Chem*. **2013**, *85*, 11960-11965.

(25) Anand, R. K.; Laws, D. R.; Chow, K.; Chang, B. Y.; Crooks, J. A.; Crooks, R. M. *Anal. Chem*. **2010**, *82*, 8766-8774.

(26) Fosdick, S. E.; Knust, K. N.; Scida, K.; Crooks, R. M. *Angew. Chem*. **2013**, *52*, 10438-10456.

(27) Rusling, J. F.; Kumar, C. V.; Gutkind, J. S.; Patel, V. *Analyst*. **2010**, *135*, 2496-2511.

(28) Muegge, B. D.; Richter, M. M.; *Anal. Chem.* **2004**, *76*, 73-77.

(29) Doeven, E. H.; Zammit, E. M.; Barbante, G. J.; Francis, P. S.; Barnett, N. W.; Hogan, C. F. *Chem. Sci.* **2013**, *4*, 977-982.

(30) Bard, A. J.; Faulker, L. R. *Electrochemical Methods Fundamentals and Applications, 2nd ed.; Wiley: New York,* **2001**.

(31) Hasheminejad, M. H.; Fang, Y.; Li, M.; Jiang, Y.; Wang, W.; Chen, H. Y. *Angew. Chem*. **2017**,

56, 1629-1633.

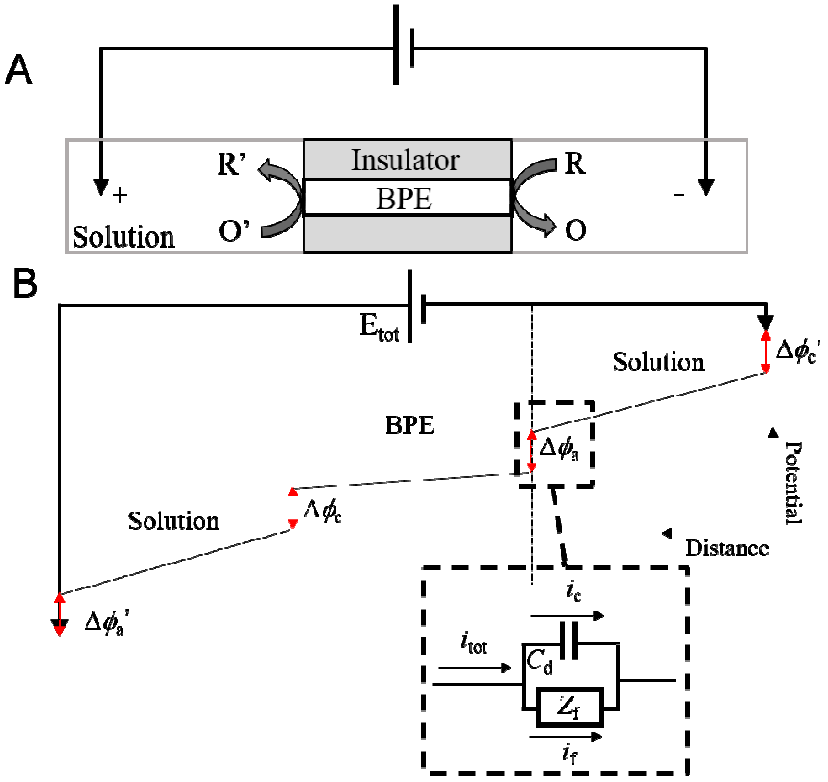

Scheme 1. (A) Schematic illustration of a closed BPE system. (B) Potential profile across the whole cell. Enlarged part shows the equivalent circuit of the anodic interface of the BPE. $\Delta\phi_a$ and $\Delta\phi_c$ represent the interfacial potential differences at the anode/solution and cathode/solution of the BPE, respectively. $\Delta\phi_a$' and $\Delta\phi_c$' represent the interfacial potential differences at the anode/solution and cathode/solution of the driving electrodes, respectively.

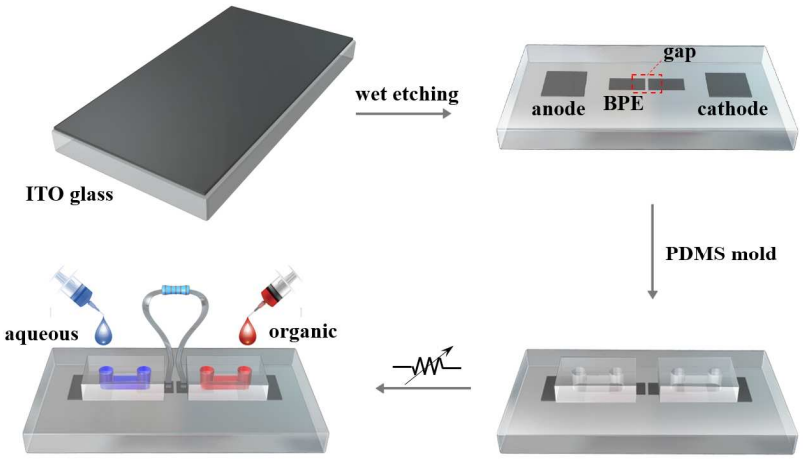

Scheme 2. The fabrication process of a closed BPE device with variable BPE resistance.

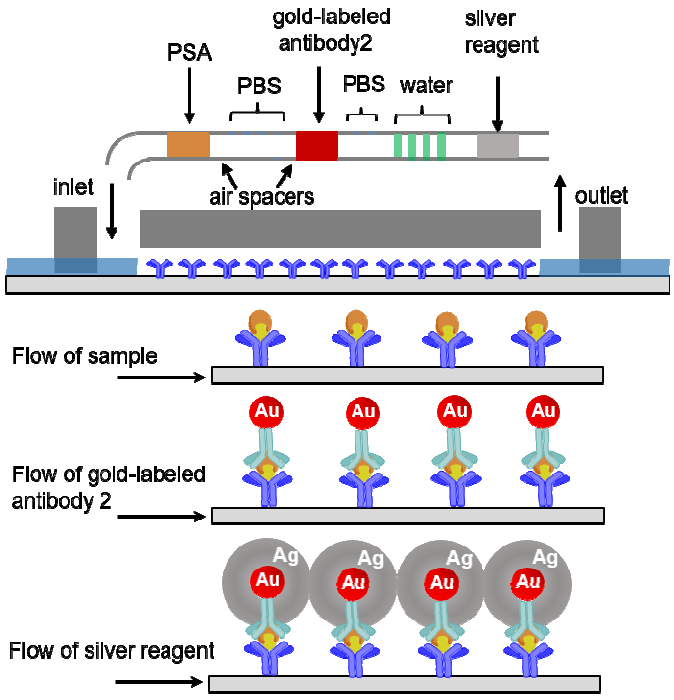

Scheme 3. Schematic diagram of passive delivery of multiple reagents, and illustration of biochemical reactions in the gap between BPEs at different immunoassay steps.

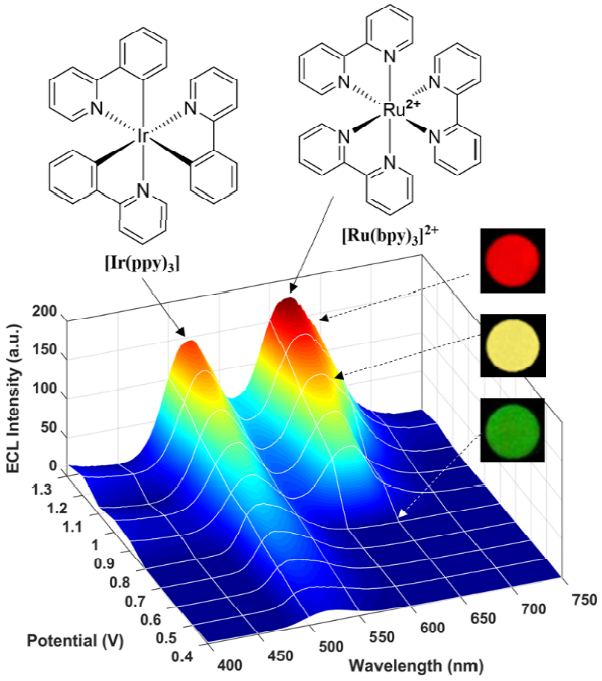

Figure 1. 3D ECL plots for a mixture of 0.5 mM $[Ir(ppy)_3]$ (λ_{max}=517 nm) and 0.75 mM $[Ru(bpy)_3]^{2+}$ (λ_{max}=620 nm), using 25 mM TPrA as the co-reactant in acetonitrile/0.1 $MTBAPF_6$. Photographs were taken at potentials of 1.3V, 1.1V and 0.8V vs. ferrocene/ferrocinium couple.

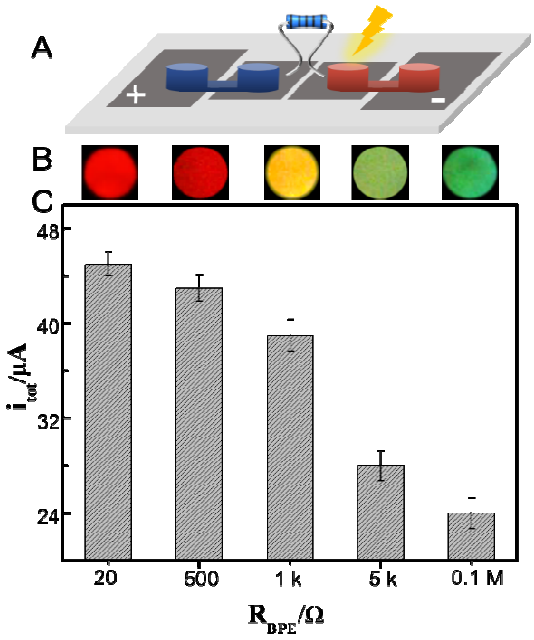

Figure 2. (A) Schematic illustration of closed BPE system using variable resistor as conductivity modulator. (B) anodic ECL image according to varied R_{BPE} from 20 Ω to 0.1 MΩ. (C) The i_{tot} in BPE circuit vs. varied R_{BPE} from 20 Ω to 0.1 MΩ. The images and currents were taken using a mixture of 0.5 mM $[Ir(ppy)_3]$ and 0.75 mM $[Ru(bpy)_3]^{2+}$ with 25 mM TPrA in acetonitrile/0.1 $MTBAPF_6$ added in the anodic reservoir at 5.5 V.

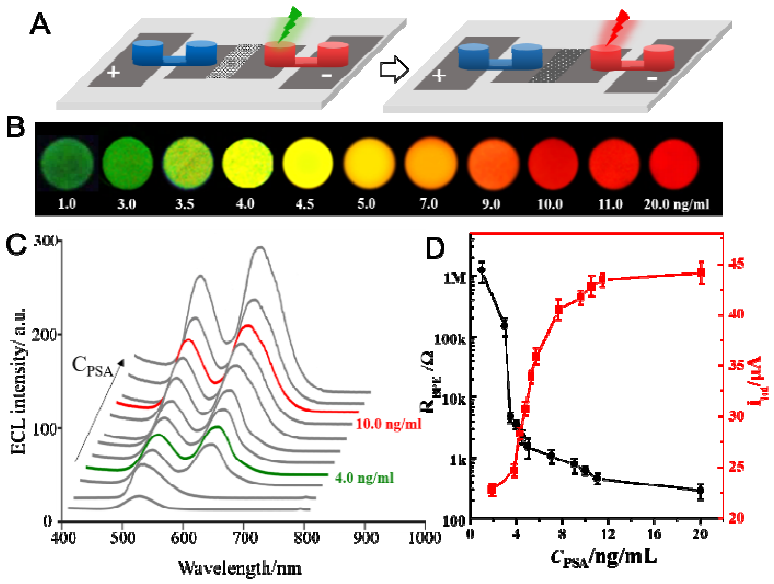

Figure 3. (A) Schematic illustration of silver bridge deposited in the gap of BPEs as conductivity modulator. (B) Photographs of the ECL at the anode of BPE with different concentrations of PSA. (C) Spooling ECL spectra with PSA concentrations from 1.0 ng/ml to 100.0 ng/ml. (D) Resistance of BPE and i_{tot} vs. PSA concentration. The images and spectra were taken using a mixture of 0.5 mM $[Ir(ppy)_3]$ and 0.75 mM $[Ru(bpy)_3]^{2+}$ with 25 mM TPrA in acetonitrile/0.1 $MTBAPF_6$ added in the anodic reservoir at 5.5 V.

Table 1. The anodic ECL images according to different blood serums

Sample	1	2	3	4	5
Clinical data(ng/ml)	1.23	6.50	9.41	10.49	16.49
ECL image					

Table of Contents